PERGAMON

Journal of Structural Geology 24 (2002) 545–556

JOURNAL OF STRUCTURAL GEOLOGY

www.elsevier.com/locate/jstrugeo

A statistic for estimating strain with confidence intervals from deformed line distributions with an application to schists and gneisses of the Western Gneiss Region, west central Norway

Kieran F. Mulchrone*

Department of Applied Mathematics, National University of Ireland, Cork, Republic of Ireland

Received 1 December 2000; revised 6 July 2001; accepted 17 July 2001

Abstract

It is shown how to calculate the axial ratio of the strain ellipse (R_s) from a deformed set of lines, assuming that they were initially uniformly distributed and deformed passively, using an exact but simple relationship between R_s and the mean resultant length ($\bar{R}$) of the distribution. The method applies to distributions of lines modified under a general 2D deformation ($-\infty < W_k < \infty$), where W_k is the kinematical vorticity number. By using the circular variance for circular data, expressions for confidence intervals and confidence levels are calculated for strain-modified distributions of lines. These expressions indicate that confidence interval widths decrease with increasing R_s and more importantly that the method is incapable of accurately estimating low strains. The method was applied to 18 gneiss and schist samples from Jøa, west central Norway and found to produce realistic strain estimates, which are internally consistent and concur with field relationships.

Keywords: Strain analysis; Fabrics; Statistics; Deformation; Gneisses

1. Introduction

Linear fabrics in rocks have received significant attention in the past. Objects, which may be considered as lines, are present in most deformed rocks and for this reason, a reliable method of strain estimation based on linear fabrics would be widely applicable.

The basic theory of how initially uniformly oriented distributions of passive linear (and planar) markers behave when deformed was developed by March (1932). Owens (1973) subsequently extended this theory to include initial distributions of any type and it is commonly referred to as the 'March Model'. In this model, each linear element is assumed to behave as a passive marker and to rotate to make a progressively smaller angle with the direction of principal extension. Despite the apparently impractical assumptions this model makes, it has been shown to be a relatively accurate predictor of linear fabrics (Oertel, 1970; Oertel and Curtis, 1972; Tullis and Wood, 1975; Tullis, 1976; Wood et al., 1976; Means et al., 1984).

By applying the 'March Model', frequency distributions of lines have been used to estimate strain by Sanderson (1973, 1977), Roberts and Sanderson (1974), Harvey and Laxton (1980), De Paor (1981), Sanderson and Meneilly (1981) and Soto (1991). Sanderson (1977) used the magnitude and orientation of the resultant mean vector **r** to estimate strain, whereas with a slightly simplified theory, Soto (1991) utilised the maximum frequency mode to estimate strain. De Paor (1981) related strain to the quartiles of the angular distribution, whereas Harvey and Laxton (1980) use the eigenvalues and eigenvectors of a direction cosine dispersion matrix for angular data to estimate strain in either two or three dimensions. Methods incorporating length (as opposed to orientation alone) are also available (Panozzo, 1984, 1987; Sanderson and Phillips, 1987; Wheeler, 1989), but these are not considered here. Lloyd (1983) reported a method that related the shape of a strain-modified distribution to strain.

Previous work demonstrates that for passively deforming linear elements, resulting frequency distributions will be symmetrical regardless of whether it is the result of co-axial or non-coaxial deformation (Lloyd, 1983; Fernandez, 1987), provided the initial distribution is uniform. However, Beach (1979), using non-passive belemnites as markers, related skewness (asymmetry of a frequency distribution) to non-coaxial deformation. For passive markers, Lloyd (1983) and Lloyd and Ferguson (1989) indicate that the symmetry and

* Corresponding author. Tel.: +353-21-902378; fax: +353-21-270813.
E-mail address: k.mulchrone@ucc.ie (K.F. Mulchrone).

0191-8141/02/$ - see front matter
PII: S0191-8141(01)00082-7

shape of a frequency distribution must be related to the nature of the initial distribution and not only to the mode of deformation. Asymmetric distributions may also result from the presence of an initial preferred orientation, i.e. non-uniformity or non-randomness (De Paor, 1980) in the distribution, but this is only of importance for initial preferred orientations at a high angle to the X-axis of the strain ellipse of the deformation. This fact is reflected in the differing responses of initial normal distributions to deformation depending on the orientation of the mean of the initial distribution (Sanderson, 1973; Roberts and Sanderson, 1974; Lloyd and Ferguson, 1989).

Ferguson (1979) rejected the assumption that linear elements behave passively during deformation and described the correlation of the 'March Model' and linear fabrics as purely 'fortuitous' i.e. coincidental. Others have also rejected the 'March Model' for strain estimation (Clark, 1970; Siddans, 1976, 1977). An alternative to the 'March Model', is to model the behaviour of linear elements by considering them as rigid ellipses (and ellipsoids) in a deforming Newtonian fluid (Jeffery, 1922; Ghosh and Ramberg, 1976; Freeman, 1985; Masuda et al., 1995). Numerically determined distributions of rigid ellipses presented by Masuda et al. (1995) are substantially different from distributions obtained assuming passive behaviour and indicates that the resulting distribution depends on flow kinematics as well as the form of the initial distribution.

Shelley (1989, 1995) provided a review of mechanisms for development of linear fabrics (particularly in relation to mineral distributions) in rocks. These are:

1. P-type development
   (a) Asymmetric fabric development under homogeneous plastic deformation related to:
      (i) heterogeneous deformation at the grain-scale
      (ii) dynamic re-crystallisation
      (iii) strain partitioning
2. G-type development
   (a) Competitive anisotropic growth (or solution)
3. M-type development
   (a) The 'March Model' (rotation and elongation of passive markers)
   (b) The tumbling behaviour of crystals during laminar flow of a viscous fluid
   (c) In rocks undergoing volume reduction either by water loss or solution
   (d) The cataclastic flow of mica in mylonites.

In most of the above cases mineral fabrics are not the result of the assumptions and mechanisms of the 'March Model'. For example, rigid markers, whose aspect ratio is greater than 10, may rotate as passive markers (Ghosh and Ramberg, 1976; Beach, 1979, 1982a,b; Beach and Jack, 1982; Fernandez, 1987; Passchier, 1987; Hamner, 1990). However, approximately 95% of mica grains used in shape preferred orientation studies have an aspect ratio of less than 10 and the majority have aspect ratios of less than five. Such low aspect ratios are even more pronounced in amphibole distributions. This evidence, coupled with the documented applicability of the 'March Model', suggests that the mathematical model derived from the 'March Model' accurately describes mineral fabrics, although the assumptions made in deriving the model may be questionable. That being said, there are instances where grain behaviour is passive, e.g. when marker viscosity is comparable with, or less than, that of the enclosing matrix.

In this paper a 2D mathematical model for the development of linear fabrics in rocks due to deformation of linear elements is devised and it is shown how this can be related to standard statistics of oriented data. The study was motivated by a desire to estimate the level of strain in highly deformed gneisses and schists of the Western Gneiss Region, Jøa, west central Norway (Mulchrone, 1999). The tools of the investigation are mathematical modelling, statistical analysis and application to natural examples. Much of the mathematical analyses and graphics were produced with the aid of Mathematica (Wolfram, 1990).

2. Derivation

Sanderson (1977) calculated an expression closely related to the probability density function (pdf) of a uniform distribution of lines deformed under pure shear. This pdf is re-derived here with minor differences, which make calculation of a statistic for strain easier and additionally, it is shown below that this approach actually applies to any general 2D deformation and not just the case of pure shear. It is important to note that in this derivation each line is treated as a unit vector, i.e. line orientation is used in the analysis, not line length. A pdf is a function that gives the relative probability that a linear element lies along a particular direction. For circular data pdf's have the following properties (Mardia, 1972, p. 40):

1. $f(\theta) \geq 0,\ -\infty < \theta < \infty$
2. $f(\theta + 2\pi) = f(\theta),\ -\infty < \theta < \infty$
3. $\int_0^{2\pi} f(\theta)\mathrm{d}\theta = 1$

where θ is orientation in radians and f is the pdf. The probability P that a linear element lies between two orientations (θ_1 and θ_2) is given by:

$$P = \int_{\theta_1}^{\theta_2} f(\theta)\mathrm{d}\theta \tag{1}$$

For every pdf there is a corresponding distribution function (F) defined as (Mardia, 1972, p. 39; Allen, 1978, p. 81):

$$\frac{\mathrm{d}F}{\mathrm{d}\theta} = f(\theta) \tag{2}$$

Sanderson (1977) refers to f as the frequency distribution and F as the frequency and includes an additional parameter

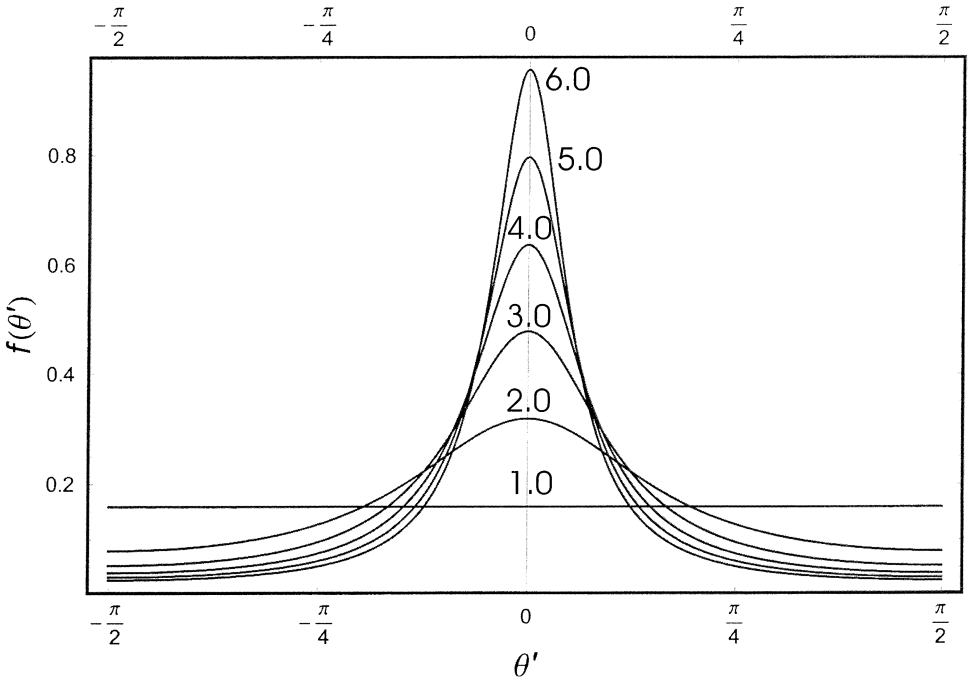

Fig. 1. Plots of the pdf, $f(\theta')$ described by Eq. (8) against θ' for $R_s = 1.0$ to 6.0.

(n) quantifying the number of lines under consideration in his analysis.

The pdf of a uniform distribution of lines is given by (Mardia, 1972, p. 50):

$$f(\theta) = \frac{1}{2\pi}, \quad -\infty < \theta < \infty \tag{3}$$

The corresponding distribution function is:

$$F(\theta) = \frac{\theta}{2\pi}, \quad -\infty < \theta < \infty \tag{4}$$

A line which initially makes an angle θ with the direction which becomes the principal extensional strain axis, makes an angle of θ' after deformation with the principal extensional strain axis. These angles are related by Wettstein's equation (Ramsay and Huber, 1983, p. 294), which is rearranged to give:

$$\theta = \tan^{-1}(R_s \tan\theta') \tag{5}$$

where R_s is the axial ratio of the finite strain ellipse. However, from elementary calculus:

$$\frac{dF}{d\theta'} = \frac{dF}{d\theta}\frac{d\theta}{d\theta'} \tag{6}$$

that is:

$$f(\theta') = f(\theta)\frac{d\theta}{d\theta'} \tag{7}$$

Differentiating Eq. (5) and substituting the result and Eq. (3) into Eq. (7) gives the pdf for a deformed uniform distribution of lines:

$$f(\theta') = \frac{1}{2\pi(R_s \sin^2\theta' + R_s^{-1}\cos^2\theta')} \tag{8}$$

This is the equivalent of Eq. 4 of Sanderson (1977) with n set equal to one.

Fig. 1 graphically illustrates the pdf resulting from pure shear deformation of initially uniformly distributed lines. A preferred orientation is symmetrically distributed around the principal extension axes of the strain ellipse, which is taken to parallel 0°. The variability of the distribution decreases with increasing strain and the distribution becomes leptokurtic.

Sanderson (1977) proposed that the statistic $|\mathbf{r}|/n$ termed the mean resultant length (Fisher, 1993, p. 32), where $\mathbf{r}$ is the resultant length of applying vector addition to a set of n lines, is useful for estimating strain. Furthermore, he presented a graph of a numerically-derived relationship between R_s and $|\mathbf{r}|/n$. Perhaps the reason that this relationship appears to have gone unnoticed by later researchers (e.g. Masuda et al., 1999) is that it is numerical and not analytical.

Following Mardia (1972, p. 20), the mean resultant length $\bar{R}$ for a discrete set of n deformed lines each of orientation θ_i' is defined as:

$$\bar{R} = \sqrt{\left(\frac{1}{n}\sum_{i=1}^{n}\cos\theta_i'\right)^2 + \left(\frac{1}{n}\sum_{i=1}^{n}\sin\theta_i'\right)^2} \tag{9}$$

The corresponding definition, in terms of the pdf in

Eq. (8) is:

$$\bar{R} = \sqrt{\left(\int_0^{2\pi} \cos\theta' f(\theta'/2)\mathrm{d}\theta'\right)^2 + \left(\int_0^{2\pi} \sin\theta' f(\theta'/2)\mathrm{d}\theta'\right)^2} \tag{10}$$

Notice that θ' is halved in the pdf. This is because oriented lines are axial, i.e. a line oriented at 25° is equivalent to a line oriented at 205°, whereas most circular statistics deal with the case where two such lines are intrinsically different, this is sometimes referred to as the cross-over problem (Fisher, 1993, p. 31). The standard procedure for dealing with such data is to double all data so that they lie between 0 and 2π, hence θ' is halved in Eq. (10) to take account of this procedure. Upon substitution of Eq. (8) into Eq. (10) the following simple expression relating R_s and $\bar{R}$ is derived:

$$R_s = \frac{1+\bar{R}}{1-\bar{R}} \tag{11}$$

where $\bar{R}$ takes on values in the range zero to one. This is the analytical relationship corresponding to Sanderson's (1977) numerical relationship. Therefore given any discrete set of lines, assumed to be initially uniformly distributed, the amount of strain incurred may be readily calculated using Eq. (11). By simplification of an equation given by Harvey and Laxton (1980), Lisle (1994) has derived an expression almost identical to Eq. (11), which is written in terms of the number of data and the resultant length (Fisher, 1993, p. 32).

Although Wettstein's equation is normally quoted with reference to pure shear deformation, the pdf derived above using Wettstein's equation applies to all initially uniform line distributions produced by general 2D deformations ($-\infty < W_k < \infty$). This is because any homogeneous constant volume deformation can be expressed as a pure shear deformation together with a rigid body rotation and translation (Hobbs et al., 1976, p. 31). More formally, suppose a displacement vector $\mathbf{X}$ transforms to $\mathbf{x}$ due to deformation, then the deformation gradient tensor $\mathbf{F} = \mathrm{d}x_i/\mathrm{d}X_j$, relates these two vectors by:

$$\mathbf{x} = \mathbf{F}\mathbf{X} \tag{12}$$

however, by the polar decomposition theorem (due to Cauchy) $\mathbf{F}$ may be uniquely decomposed as follows:

$$\mathbf{F} = \mathbf{R}\mathbf{U} = \mathbf{V}\mathbf{R} \tag{13}$$

where $\mathbf{R}$ is a proper orthogonal tensor (i.e. a rigid body rotation) and $\mathbf{U}$ and $\mathbf{V}$ are the symmetric right and left stretch tensors (pure shear), respectively (Lai et al., 1993, pp. 124–125). Moreover, this theorem proves that any general deformation can be decomposed into rigid body rotation and a pure shear deformation. As pointed out by Owens (1973) and Sanderson and Meneilly (1981), the rigid body rotation part (i.e. $\mathbf{R}$) of a deformation has no affect on an initially uniform line distribution so that the after deformation line distribution is equivalent to a rotated pure shear (Wettstein) distribution. Hence, the pdf derived for strain-modified distributions (Eq. (8)) using Wettstein's equation and Eq. (11) may be applied to distributions of lines produced by any general 2D deformation.

3. Confidence interval

Circular variance (S_0) is a common measure of dispersion for circular data (Mardia, 1972, p. 22; Fisher, 1993, p. 32) and is defined as follows:

$$S_0 = 1 - \bar{R} \tag{14}$$

If this statistic is to be useful at all, the percentage confidence that the estimated value of $\bar{R}$ lies within the range ($\pm NS_0$) needs to be known where N is a positive integer. The confidence level (CL) may be calculated using the pdf in Eq. (8) as follows:

$$CL = 100\int_{-NS_0}^{NS_0} f(\theta'/2)\mathrm{d}\theta' \tag{15}$$

note that θ' is halved in the pdf due to the cross-over problem associated with axial data and the integral is multiplied by 100 to make the result a percentage. By substituting $\bar{R} = (R_s - 1)/(R_s + 1)$ this evaluates to:

$$CL = \frac{200}{\pi}\tan^{-1}\left(R_s \tan\left(\frac{\mathrm{N}}{1+R_s}\right)\right) \tag{16}$$

So that we may be $CL\%$ confident that R_s lies within the range ($R_s - NS_0$, $R_s + NS_0$).

Caution is advised when applying Eq. (16) as this function is not well behaved for low R_s values. This is because for low R_s values, $|NS_0| > \pi/2$, which is outside the range of axial data, i.e. ($-\pi/2$, $\pi/2$) implying 100% confidence that R_s lies within the range ($R_s - NS_0$, $R_s + NS_0$). CL is investigated graphically in Fig. 2 for $N = 3$, 5 and 7. When $N = 3$ or 5, Eq. (16) is well behaved for $R_s \gtrapprox 2.2$, so that

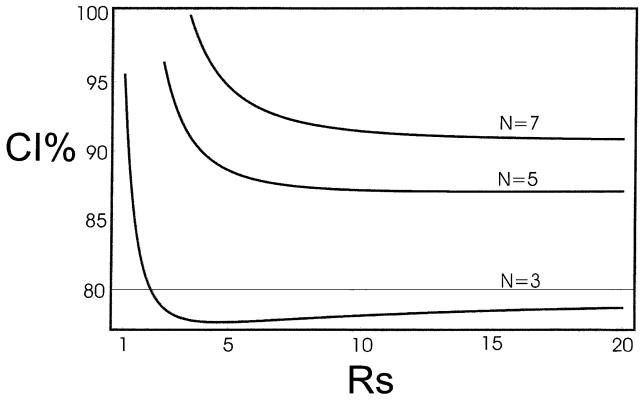

Fig. 2. CI as a function of R_s for $N = 3$,5 and 7. Notice that CI increases as R_s increases and that for $N = 3$, $CI > 75\%$ and for $N = 5$, $CI > 85\%$ and for $N = 7$, $CI > 90\%$.

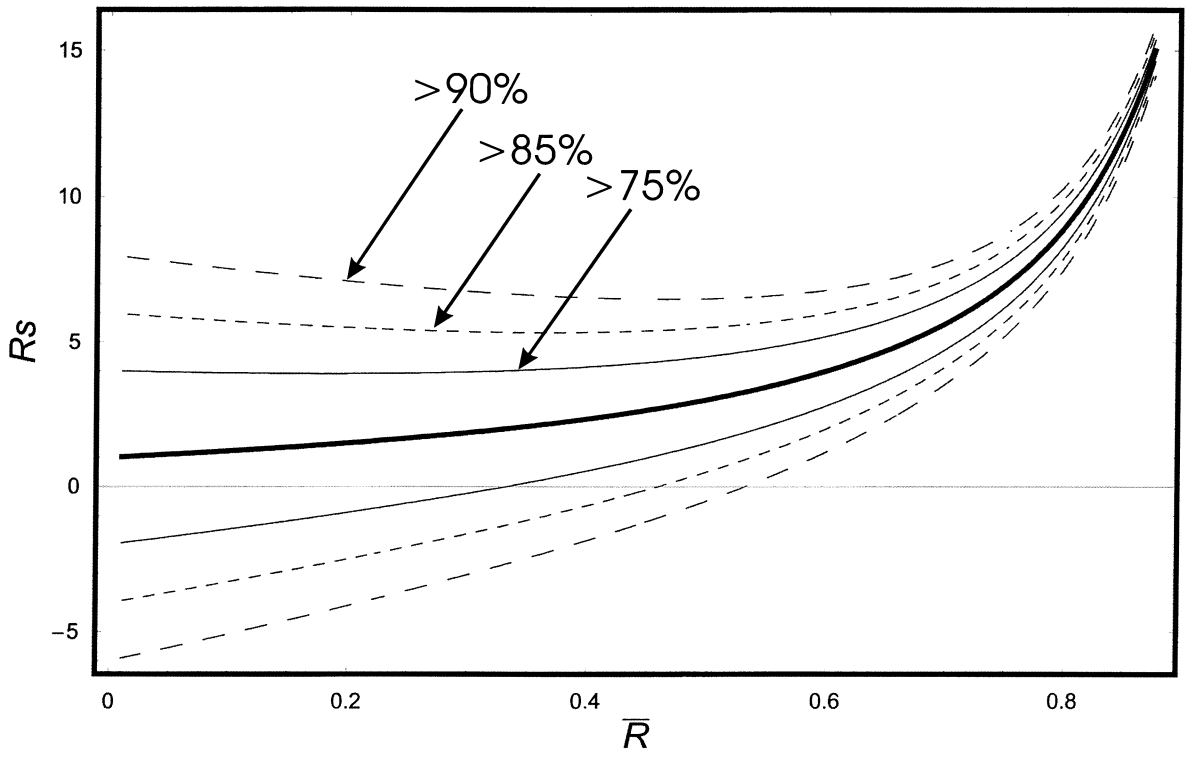

Fig. 3. Graph of R_s versus $\bar{R}$ as determined from Eq. (11) with confidence intervals.

$CL \approx 100\%$ for $R_s \lessapprox 2.2$, whereas for $N = 7$, CL is approximately equal to 100% for $R_s \lessapprox 3.5$. It is noted that confidence increases for increasing values of R_s and that $N = 3$ represents the >75% confidence interval, $N = 5$ the >85% confidence interval and $N = 7$ the >90% confidence interval.

Fig. 3 shows Eq. (11) together with confidence intervals calculated with Eq. (14). Confidence interval width decreases rapidly with increasing R_s, indicating that strain values calculated using Eq. (11) are accurate over a wide range of $\bar{R}$ values. Furthermore, it shows that the method is incapable of detecting small strain values (i.e. the confidence interval includes $R_s = 1$). For example, at the >90% confidence interval calculated strain values must be greater than 4.1 before it can be confidently asserted that this value differs significantly from $R_s = 1$. However at the >75% and >85% confidence levels the method is capable of detecting strains greater than 2.7 and 3.3, respectively.

4. Application to the western gneiss region, west central Norway

4.1. Geological setting

The study area is located on the island of Jøa, west central Norway (Fig. 4). Jøa forms part of Vestranden, the northern portion of the Western Gneiss Region (WGR) (Schouenborg, 1986, 1988; Johansson et al., 1987; Möller, 1988), which consists largely of granitic and granodioritic migmatised gneisses and local occurrences of diorite, monzodiorite, monzonite and charnockite (Möller, 1988). Many infolded sequences of metasediments consisting of psammites, pelites, marbles, calcsilicates and metavolcanics, have been identified (e.g. Ramberg, 1943; Andréasson and Johansson, 1983; Schouenborg, 1986, 1988, 1989; Tucker, 1986; Johansson et al., 1987; Möller, 1988; Piasecki and Cliff, 1988). Most metasediments are thought to be allochthonous (Schouenborg 1986, 1988; Johansson et al., 1987; Möller, 1988), however, authochthonous sequences have also been observed (Schouenborg, 1989).

On Jøa, four distinct lithological associations have been identified and mapped (Mulchrone, 1999; see Fig. 5). The Doubly Migmatised Gneiss Association (DMGA) consists of intensely deformed heterogeneous gneisses with two generations of leucosome and multiple episodes of intrusion, two of which are mafic. A large body of deformed homogeneous orthogneisses, with one generation of leucosome and a single suite of mafic intrusives, intrudes the DMGA and is termed the Singly Migmatised Gneiss Association (SMGA). Mafic dykes and bodies are grouped together into the Mafic Intrusive Association (MIA), which represents multiple episodes of mafic intrusive activity. Partially enclosed in the DMGA, the Metasedimentary Schist Association (MSA) consists of a sequence of semi-pelitic schists, psammites, quartzites, calc-schists,

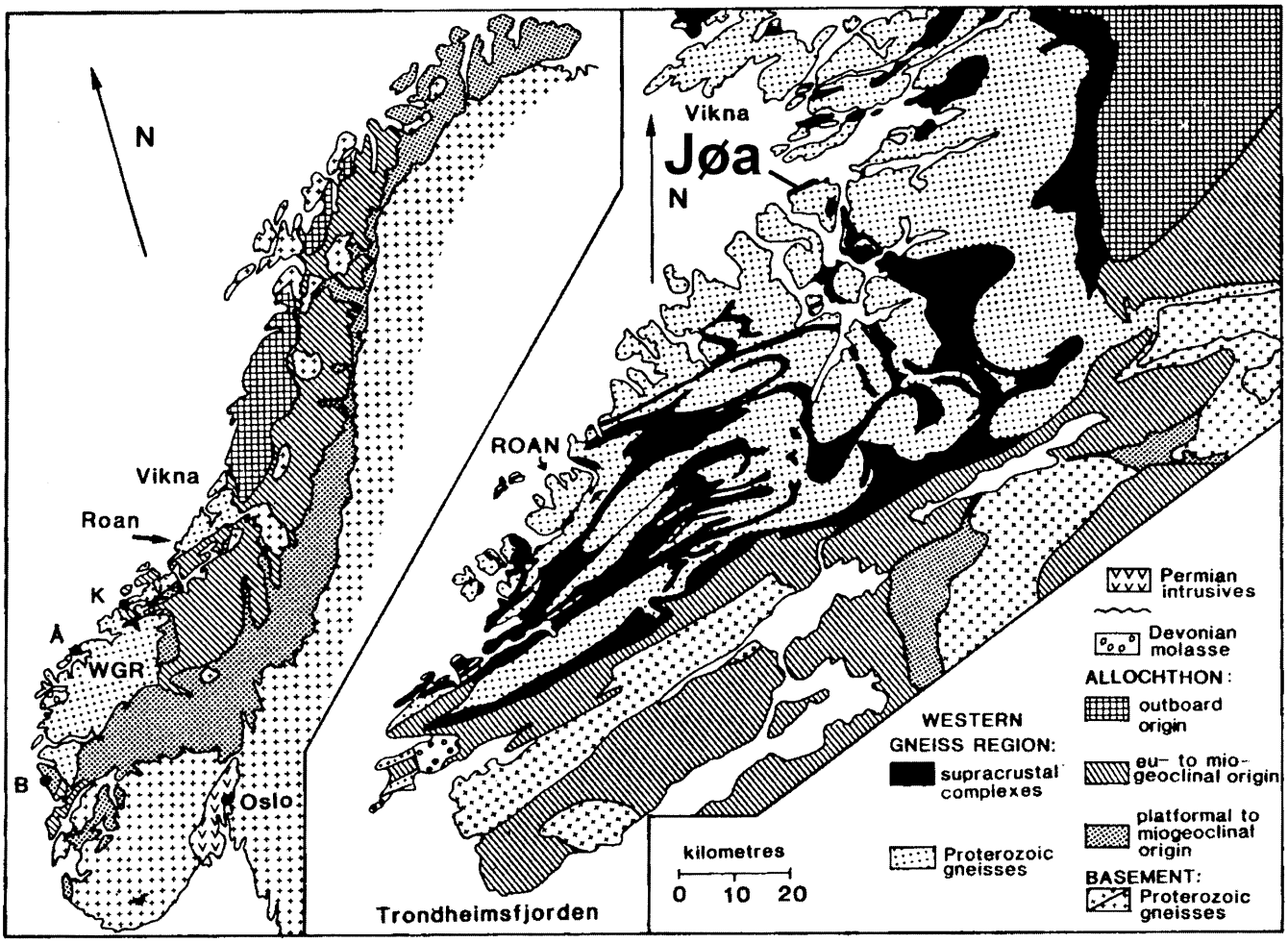

Fig. 4. General geology of the WGR of Vestranden in west central Norway. The location of the island of Jøa is indicated.

calcsilicate schists and marbles, from which leucosome, mafic dykes and pegmatitic dykes are totally absent.

A complex structural, metamorphic and intrusive history has been unravelled for the area (Mulchrone, 1999). A schematic illustration of the history of the area is presented in Fig. 6. During the Svecofennian the DMGA protolith formed by intrusion of acid, intermediate and mafic bodies into pre-existing sediments. The DMGA was subjected to at least one, probably two episodes of deformation (termed D_{n-2} and D_{n-1}) and underwent migmatisation (LC_1) prior to intrusion of the SMGA at around 1650 Ma. Further mafic intrusive activity occurred prior to development of a pervasive foliation (S_n) in the DMGA, SMGA and MIA, during D_n, an intense episode of Caledonian deformation c. 440 Ma ago, formed by amphibolite facies recrystallisation of hornblende and biotite, which obliterated all pre-existing fabrics. S_n was overprinted by blastesis of felsic minerals during Caledonian migmatisation and leucosome development (LC_2) c. 430 Ma, i.e. peak thermal conditions, which was coeval with D_{n+1} deformation in the basement (DMGA, SMGA and MIA), identified from mesoscale folding and shearing of S_n. Thrust emplacement of the MSA onto the basement at around 400 Ma was accompanied by amphibolite facies S_{n+2} foliation development in the MSA and growth of garnet blasts in both the MSA and the basement, which is postulated to reflect a temporary increase in pressure at this time. Minor folding of S_{n+2} in the MSA is ascribed to a later generation of deformation (S_{n+3}). The basement is unaffected by D_{n+2} and D_{n+3} and appears to have been less ductile than the MSA at this time. Later stage map-scale folding has folded S_n in the basement together with S_{n+2} in the MSA into large isoclinal folds with reclined axial surfaces and fold axes plunging moderately to the east, which are correlated with regional large-scale folding in Vestranden and are probably of Early Devonian age.

4.2. Methods

Eighteen samples of micaceous schists and gneisses were studied in order to investigate strain levels. Due to the complex lithological, structural and metamorphic history determined for these rocks, it was felt that production of a strain map for the area would be of uncertain value and therefore samples are not oriented but are sectioned normal

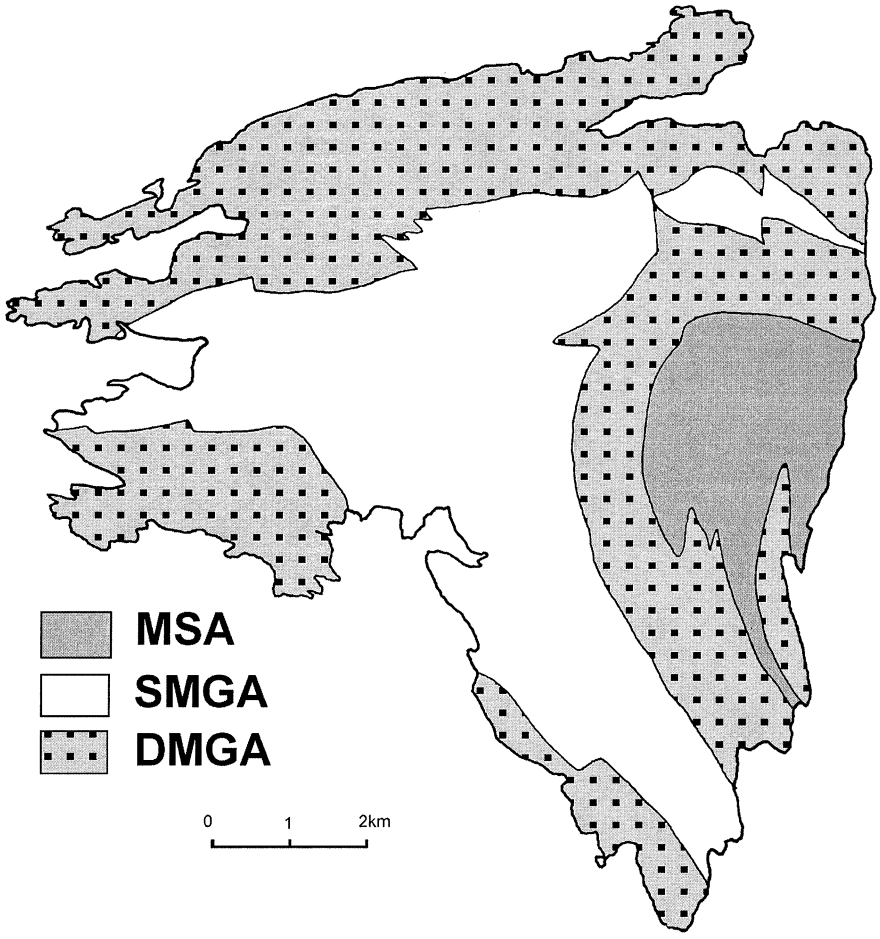

Fig. 5. A simplified geological map of Jøa with the pattern of the DMGA, SMGA and MSA shown. The MIA does not occur in large-scale mappable units.

to the main rock fabric (S_n) and parallel to the lineation (L_n within the plane of S_n), if one was present.

The linear elements used in the vast majority of the analyses were biotite and hornblende, and because the statistical method developed above assumes passive rotation of linear markers, it is necessary to justify that this assumption applies to biotite and hornblende in a quartzofeldspathic matrix. Biotite was used as the linear marker in most cases and it was found that approximately 100 measurements per sample produced stable results. The length, width, aspect ratio and orientation of biotite grains were measured for four of the samples investigated WGC/88/22; WGR/90/1; WGR/90/2 and WGR/90/3 (Fig. 7). Aspect ratios are between two and eight, which lies outside the limit of 7–10 for passive behaviour (Ghosh and Ramberg, 1976; Passchier, 1987; Hamner, 1990), although this limit applies only to rigid objects. Biotite and micas in general do not deform in a rigid fashion (Passchier and Trouw, 1996, p. 50). In the samples investigated, biotite grains are readily observed to exhibit characteristics indicative of internal deformation, including undulose extinction, kinking, microfolding or possible gliding along the basal plane (001). It is suggested that biotite deformed in order to accommodate strain imposed by the surrounding matrix, a situation incompatible with a rigid body hypothesis. Therefore it is argued that biotite did not behave as a rigid marker and thus the aspect ratio limit of 10 is probably too high for biotite.

In addition, biotite used in the analysis is always embedded in a quartzofeldspathic matrix and it is thought that the relative competency contrast between biotite and this matrix is low. This contention is supported by the common observation that in zones of intense deformation biotite grainsize is reduced, whereas feldspar behaves rigidly. Although quartz also undergoes a grainsize reduction, it is thought unlikely that biotite behaves rigidly with respect to its surrounding matrix. This implies that biotite behaviour is constrained by matrix behaviour, as evidenced by microscopic biotite deformation and should rotate passively. Its internal modes of deformation (e.g. basal gliding) tend to comply with the external constraints of matrix deformation.

Means et al. (1984) experimentally investigated the behaviour of micas and their analysis concurs with the above assertion. The initial mica distribution was not uniform but traces of 001 were preferentially oriented parallel to the compression direction. They found that at low strains, the ‘March Model’ (passive behaviour)

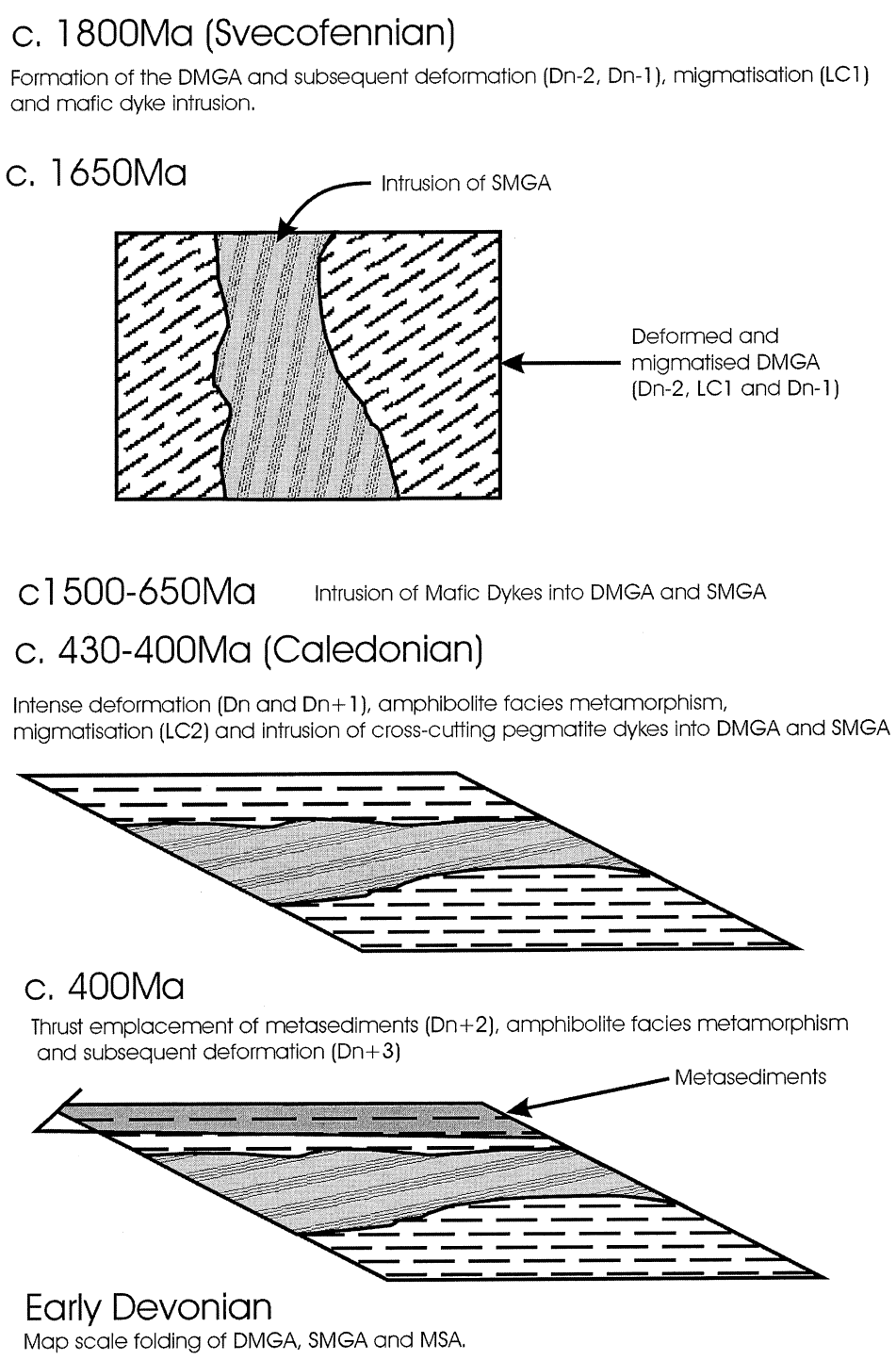

Fig. 6. A schematic representation of the structural, metamorphic and migmatic history of the rock sequence on Jøa.

underestimated the amount of rotation, whereas the reverse was true at higher strains. However, in all cases, resulting distributions were comparable with the 'March Model'. Differences between observation and the 'March Model' were accounted for by kinking and folding of grains sub-parallel to the compression direction. This effect is less pronounced in initially uniform distributions because a small proportion of grains initially parallel the compression direction. Grains close to the extension direction rotate passively, whereas those close to the compression direction tend to kink. Thus it is considered reasonable to assume that the biotite studied here behaved passively during deformation (i.e. its behaviour approximates to the 'March Model').

Hornblende was used as a linear marker in WGC/88/22 and aspect ratios are presented in Fig. 7. Aspect ratios range

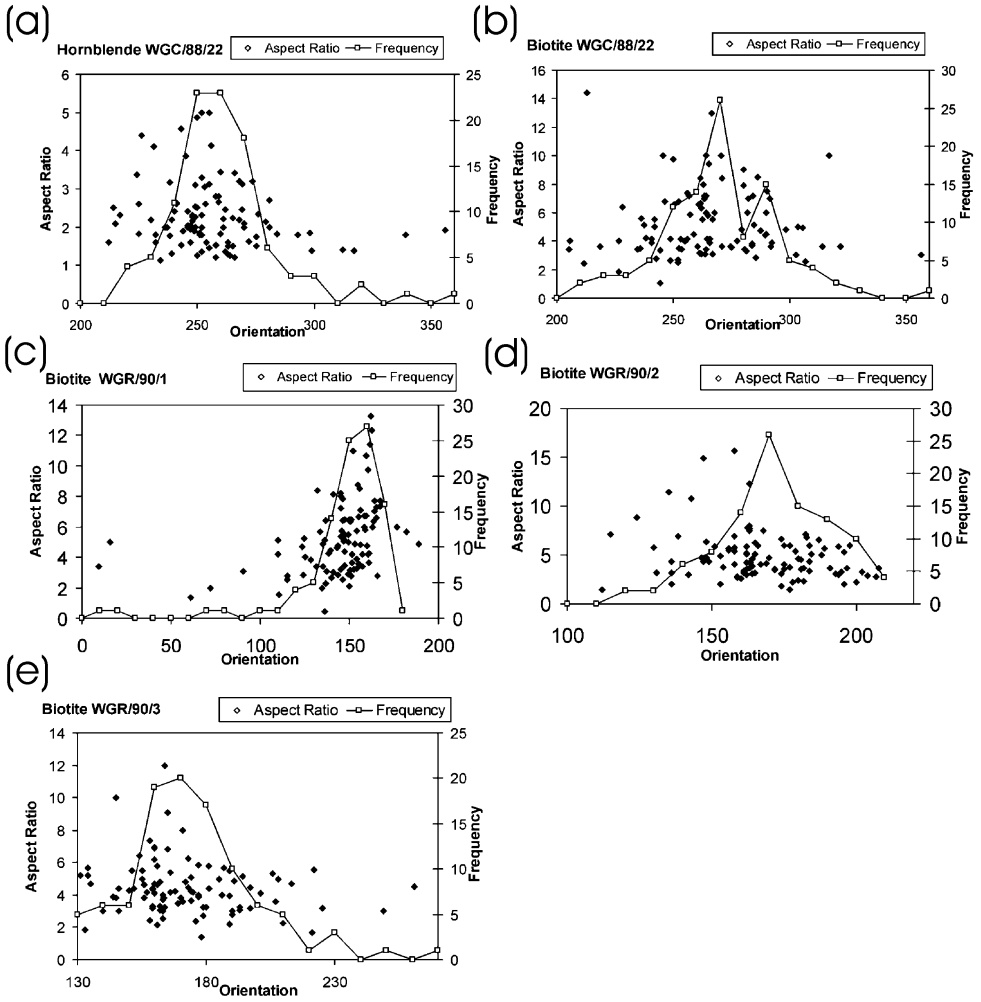

Fig. 7. Plots of aspect ratio and frequency distribution for five representative samples.

Table 1
Results of the analysis for 18 samples from Jøa

Sample	n	Mean	Mode	$\bar{R}$	R_s	$> 90\%$	R_s (Soto)	Group
WGC/88/13	102	184.6	185.0	0.79	8.52	± 1.47	5.12	DMGA
WGC/88/19	102	178.0	159.0	0.85	12.33	± 1.05	4.76	MIA
WGC/88/22(B)	101	264.0	265.5	0.69	5.45	± 2.17	4.68	MIA
WGC/88/22(H)	100	253.3	252.0	0.77	7.70	± 1.61	4.14	MIA
WGC/88/23	101	182.0	201.0	0.68	5.25	± 2.24	3.00	DMGA
WGC/88/3	103	155.0	139.0	0.55	3.44	± 3.15	4.02	DMGA
WGC/88/41	102	175.7	189.0	0.63	4.41	± 2.59	3.00	MSA
WGC/88/43	100	154.0	152.0	0.69	5.45	± 2.17	3.78	MSA
WGC/88/44	101	182.0	176.0	0.94	32.33	± 0.42	6.41	MSA
WGC/88/55	100	177.5	157.0	0.43	2.51	± 3.99	2.34	SMGA
WGC/88/68	103	285.8	288.0	0.88	15.67	± 0.84	5.94	DMGA
WGC/88/10(L)	101	190.5	184	0.75	7.00	± 1.75	4.63	DMGA
WGC/88/10(M)	101	196.5	202	0.84	11.50	± 1.12	4.27	DMGA
WGR/89/32	102	168.4	160	0.91	21.22	± 0.63	6.53	MIA
WGR/90/1	100	148.7	146.4	0.81	9.53	± 1.33	4.86	MSA
WGR/90/2	100	167.6	162.0	0.78	8.09	± 1.54	4.68	DMGA
WGR/90/3	100	167.8	160	0.70	5.67	± 2.10	3.60	MSA
WGR/76	102	167.0	181	0.76	7.33	± 1.68	3.78	DMGA

from one to six but the majority of grains have aspect ratios of around two. This is well below the limit of 7–10. Bard (1985, p. 85) and Passchier and Trouw (1996, p. 51) indicate that hornblende behaves rather rigidly during deformation and distributions may not be well modelled by the 'March Model'. As such, it is probable that hornblende behaved in a non-passive manner during deformation and resulting distributions may be better interpreted using the results of Masuda et al. (1995).

4.3. Results

Frequency distributions and aspect ratios for five samples are presented in Fig. 7 and statistics calculated for all 18 samples are presented in Table 1. Many samples exhibit a high degree of skewness indicated by differing orientations of the mean and mode, although half are symmetric (WGC/88/13, 22(B), 22(H), 43 and 68) or only mildly asymmetric (WGC/88/44, WGR/90/1, 2). Asymmetric distributions could be the result of non-uniform initial distributions, multiple deformation episodes, non-passive behaviour or syn-tectonic recrystallisation. In any case, it suggests that the results obtained from the method developed here should be treated as first order estimates. In Fig. 7 a correlation between high aspect ratio values and orientation with respect to the frequency maximum is clear. This is the result of enhanced crystal growth along the length of grains of a suitable orientation as there is no evidence to suggest tectonic stretching of crystals.

The mean resultant length $\bar{R}$ was calculated according to Eq. (9) and subsequently Eq. (11), derived above, was applied to obtain strain estimates. In addition, the method of Soto (1991) was also applied to obtain additional estimates. Using Eq. (11) most strain (R_s) values lie between four and 10 with extreme values of 20–30. Application of Soto's (1991) method almost always gives lower strain estimates. Soto's (1991) method uses the frequency maximum (i.e. a subset of the data) to estimate strain, whereas application of Eq. (11) takes into account all data. This may account for differences in calculated values. Application of Eq. (11) is better because:

1. The method developed here is a sufficient statistic (Castella and Berger, 1990, p. 247) whereas Soto's method is not. In general, any technique that uses all available data is preferable to a method using only a subset of the data and is almost always the most efficient statistic possible.
2. Soto's method involves selecting a subset of the data based on an interval of arbitrary size. Different strain estimates may be calculated depending on the location and size of interval used and therefore Soto's method is less robust than the method developed here, because one strain estimate is produced for each data set.

Many of the samples studied display asymmetric distributions indicated by significantly different values for mean and mode (Table 1). Eq. (11) was derived under the assumption of an initially uniform distribution deformed by a general 2D deformation, which always results in symmetric final distributions (Lloyd, 1983; Fernandez, 1987). To explain these asymmetric distributions it is noted that in samples from the DMGA and SMGA biotite defines the S_n foliation and recrystallised immediately prior to or coeval with D_n. Likewise, biotite crystals from MSA samples define S_{n+2} and recrystallised immediately prior to or coeval with D_{n+2}. Therefore these distributions are unlikely to have developed due to interference of multiple deformation episodes, which can result in asymmetric distributions (De Paor, 1980). However, pre-existing fabrics may have lead to preferential recrystallisation and growth. It must be emphasised that the strain estimate calculated using Eq. (11) for asymmetric distributions represent at best first order estimates for the true value of R_s as a fundamental assumption of the method is clearly violated.

WGC/88/22 was analysed using both biotite and hornblende. Both distributions are symmetric, but the strain estimate using hornblende is significantly greater than that calculated using biotite. Petrological studies (Mulchrone, 1999) indicate that biotite probably post dates hornblende, which may account for the higher R_s value obtained from hornblende. The differing values may also be related to differing modes of behaviour, i.e. passive biotite and non-passive hornblende.

Both leucosome (LC_2) and mesosome biotite distributions were measured and analysed separately for sample WGC/89/10. The resulting distributions are similar, although the strain estimate is considerably higher for the mesosome distribution i.e. 11.50 ± 1.12 compared with 7.00 ± 1.75. This result is consistent with field relationships indicating that LC_2 leucosome post-dates D_n and is broadly synchronous with D_{n+1}. The results of the analysis confirm that the mesosome has undergone a longer deformation history than LC_2, but also suggests that D_n fabrics underwent significant modification during D_{n+1}.

As mentioned earlier, making broad statements about large-scale strain patterns on the basis of such limited data is dangerous considering the complex structural, metamorphic, intrusive and migmatitic history determined for Jøa. Lithology and intensity of deformation can vary rapidly at outcrop scale not to mention even larger scales. However, on the basis of the data available (see Table 1) average R_s in the DMGA is ≈ 8.0, which probably includes contributions from both D_n and D_{n+1}. A single sample from the SMGA gives a relatively low R_s value, possibly indicating that this large homogeneous orthogneissic body behaved in a less ductile manner than the surrounding heterogeneous DMGA during D_n and D_{n+1}. Strain values from the MSA due to D_{n+2} and D_{n+3} are of the same order as those from the DMGA, except for one extremely large value, which may be indicative of localised intense deformation possibly related to internal thrusting. Field relationships constrain thrust

emplacement (syn-D_{n+2}) of the MSA to be post-D_{n+1} deformation and LC_2 migmatisation in the basement, so these strain estimates provide evidence for passive basement behaviour during both D_{n+2} and D_{n+3}. Otherwise the basement should exhibit higher strains than the MSA. R_s values from the MIA are larger, on average, than those in the other associations, but this is probably due to strain localisation due to competency contrast between mafic lithologies of the MIA and their enclosing gneisses.

5. Discussion and conclusions

When working in highly deformed, metamorphosed and migmatised rocks such as those of the WGR, a quick review of the strain-analysis literature, indicates quite clearly that the majority of strain analysis techniques do not apply. Although the method of Talbot (1970) is useful, it depends on the presence of suitably oriented deformed veins, a feature which was not abundant on Jøa. Alternatively the R_f/ϕ method (Ramsay, 1967, pp. 202–211) may be applied to augen gneisses. However, on Jøa augen gneiss does not occur in enough abundance to be of use in strain analysis. Therefore from the perspective of the WGR, as exposed on Jøa, there was a clear need for a widely applicable, reliable and relatively speedy method of strain estimation.

It is suggested that the method derived in this paper is such a method because:

1. It is widely applicable as it only requires the presence of mica in a quartzofeldspathic matrix.
2. It is reliable due to the availability of confidence levels and intervals, provided the fundamental assumptions used to develop the method can be justified.
3. It is speedy because once a thin section is available strain estimates can be calculated within 10–20 min.

In conclusion, an exact analytical relationship between the axial ratio of the strain ellipse (R_s) and the mean resultant length ($\bar{R}$) of a deformed set of initially uniformly distributed set of lines was derived. The derived relationship is algebraically simple and applies to distributions modified under general 2D deformation regimes. Using the circular variance for circular data expressions for confidence intervals and confidence levels are calculated for strain modified distributions of lines. This indicates that confidence interval widths decrease with increasing R_s and more importantly that the method is incapable of accurately estimating low strains.

The method of this paper and that of Soto (1991) was applied to 18 gneiss and schist samples from Jøa, west central Norway. The method of Soto (1991) was shown to underestimate strain-values probably because only a subset of the data were used in that analysis, whereas the full data set is used in the method presented in this paper. Strain values calculated from the samples are realistic, internally consistent and concur with field relationships.

Acknowledgements

Field work for this study was sponsored by Norsk Geologiske Undersøkelse, Trondheim and is gratefully acknowledged. I thank Dr A.R. Allen, Geology, NUI, Cork for help and encouragement during this work. I also thank Ms Kathleen O' Sullivan, Director, Statistical Laboratory, NUI, Cork and Dr Patrick A. Meere, Geology, NUI, Cork for reviewing and improving an early draft of the manuscript. Thorough and critical reviews by Drs R.J. Lisle and G.E. Lloyd greatly improved this work.

References

Allen, A.O., 1978. Probability, Statistics, and Queueing Theory. Academic Press, Orlando, FL.

Andréasson, P.G., Johnansson, L., 1983. The Snåsa Mega-lens, west central Scandinavian Caledonides. Geologiska Föreningens i Stockholm Förhandlinar 102, 335–357.

Bard, J.P., 1985. Microtextures of Igneous and Metamorphic Rocks. D. Reidel Publishing Company, Lancaster.

Beach, A., 1979. The analysis of deformed belemnites. Journal of Structural Geology 1, 127–135.

Beach, A., 1982a. Deformation mechanisms in some cover thrust sheets from the external French Alps. Journal of Structural Geology 4, 137–149.

Beach, A., 1982b. Strain analysis in a cover thrust zone, external French Alps. Tectonophysics 88, 333–346.

Beach, A., Jack, S., 1982. Syntectonic vein development in a thrust sheet from the external French Alps. Tectonophysics 81, 67–84.

Castella, G., Berger, R.L., 1990. Statistical Inference. Duxbury Press, Belmont, CA.

Clark, B.R., 1970. Mechanical formation of preferred orientation in clays. American Journal of Science 269, 250–266.

De Paor, D.G., 1980. Some limitations of the R_f/ϕ technique of strain analysis. Tectonophysics 64, T29–T31.

De Paor, D.G., 1981. Strain analysis using deformed line distributions. Tectonophysics 73, T9–T14.

Ferguson, C.C., 1979. Rotations of elongate rigid particles in slow non-newtonian flows. Tectonophysics 60, 247–262.

Fernandez, A., 1987. Preferred orientation developed by rigid markers in two-dimensional simple shear strain: a theoretical and experimental study. Tectonophysics 136, 151–158.

Fisher, N.I., 1993. Statistical Analysis of Circular Data. Cambridge University Press, Cambridge, UK.

Freeman, B., 1985. The motion of rigid ellipsoidal particles in slow flows. Tectonophysics 113, 163–183.

Ghosh, S.K., Ramberg, H., 1976. Reorientation of inclusions by combinations of pure and simple shear. Tectonophysics 34, 1–70.

Hamner, S.K., 1990. Natural rotated inclusions in non-ideal shear. Tectonophysics 176, 245–255.

Harvey, P.K., Laxton, R.R., 1980. The estimation of finite strain from the orientation distribution of passively deformed linear markers: eigenvalue relationships. Tectonophysics 70, 285–307.

Hobbs, B.E., Means, W.D., Williams, P.F., 1976. An Outline of Structural Geology. John Wiley and Sons, New York.

Jeffery, G.B., 1922. The motion of ellipsoidal particles immersed in a viscous fluid. Proceedings of the Royal Society of London A 120, 161–179.

Johansson, L., Andréasson, P.G., Schöberg, H., 1987. An occurrence of the Gula Nappe in the Western Gneiss Region, central Scandinavian Caledonides. Norsk Geologiske Tidsskrift 67, 85–92.

Lai, W.M., Rubin, D., Krempl, E., 1993. Introduction to Continuum Mechanics. Pergamon Press, Oxford.

Lisle, R.J., 1994. Paleostrain analysis. In: Hancock, P.L. (Ed.). Continental Deformation. Pergamon Press, Oxford, pp. 28–42.

Lloyd, G.E., 1983. Strain analysis using the shape of expected and observed continuous frequency distributions. Journal of Structural Geology 5, 225–231.

Lloyd, G.E., Ferguson, C.C., 1989. Belemnites, strain analysis and regional tectonics: a critical appraisal. Tectonophysics 168, 239–253.

March, A., 1932. Mathematische Theorie der Regelung nach der Korngestalt bei affiner Deformation. Z. Kristallogr. 81, 285–297.

Mardia, K.V., 1972. Statistics of Directional Data. Academic Press, London.

Masuda, T., Michibayashi, K., Ohta, H., 1995. Shape preferred orientation of rigid particles in a viscous matrix: re-evaluation to determine kinematic parameters of ductile deformation. Journal of Structural Geology 17, 115–129.

Masuda, T., Kugimiya, Y., Aoshima, I., Hara, Y., Ikea, H., 1999. A statistical approach to determination of a mineral lineation. Journal of Structural Geology 21, 467–472.

Means, W.D., Williams, P.F., Hobbs, B.E., 1984. Incremental deformation and fabric development in a KCl–mica mixture. Journal of Structural Geology 6, 378–391.

Möller, C., 1988. Geology and metamorphic evolution of the Roan area, Vestranden, Western Gneiss Region, Central Norwegian Caledonides. Norsk Geologiske Undersøkelse 413, 1–31.

Mulchrone, K.F., 1999. The geology and structure of the Western Gneiss Region, Jøa, West Central Norway. Unpublished Ph.D. Thesis, National University of Ireland, Cork.

Oertel, G., 1970. Deformation of a slaty, lapillar tuff in the Lake District, England. Geological Society of America Bulletin 81, 1173–1187.

Oertel, G., Curtis, C.D., 1972. Clay-ironstone concretion preserving fabrics due to progressive compaction. Geological Society of America Bulletin 83, 2597–2602.

Owens, W.H., 1973. Strain modification of angular density distributions. Tectonophysics 16, 249–261.

Panozzo, R., 1984. Two-dimensional strain from the orientation of lines in a plane. Journal of Structural Geology 6, 215–221.

Panozzo, R., 1987. Two-dimensional strain determination by the inverse SURFOR wheel. Journal of Structural Geology 9, 115–119.

Passchier, C.W., 1987. Stable positions of rigid objects in non-coaxial flow — a study in vorticity analysis. Journal of Structural Geology 9, 419–427.

Passchier, C.W., Trouw, R.A.J., 1996. Microtectonics. Springer Verlag, Berlin.

Piasecki, M.A.J., Cliff, R.A., 1988. Rb–Sr dating of strain-induced mineral growth in ductile shear zones in the Western Gneiss Region of Nord-Trøndelag, Central Norway. Norsk Geologiske Undersøkelse 413, 33–50.

Ramberg, H., 1943. En undersøkelse av Vestrandens regional-metamorfe bergarter. Norsk Geologiske Tidsskrift 23, 1–174.

Ramsay, J.G., 1967. Folding and Fracturing of Rocks. McGraw-Hill, New York.

Ramsay, J.G., Huber, M.I., 1983. The Techniques of Modern Structural Geology, Volume 1: Strain Analysis. Academic Press, London.

Roberts, J.L., Sanderson, D.J., 1974. Oblique fold axes in the Dalradian rocks of the Southwest Highlands. Scottish Journal of Geology 9, 281–296.

Sanderson, D.J., 1973. The development of fold axes oblique to the regional trend. Tectonophysics 16, 55–70.

Sanderson, D.J., 1977. The analysis of finite strain using lines with an initial random orientation. Tectonophysics 43, 199–211.

Sanderson, D.J., Meneilly, A.W., 1981. Analysis of three-dimensional strain modified uniform distributions: andalusite fabrics from a granite aureole. Journal of Structural Geology 3, 109–116.

Sanderson, D.J., Phillips, S.J.L., 1987. Strain analysis using length-weighting of deformed random line elements. Journal of Structural Geology 9, 511–514.

Schouenborg, B.E., 1986. An allochthonous cover in northern Vestranden, Western Gneiss Region, central Norway. Geologiska Föreningens i Stockholm Förhandlinar 108, 127–133.

Schouenborg, B.E., 1988. U/Pb-zircon datings of Caledonian cover rocks and cover-basement contacts, northern Vestranden, central Norway. Norsk Geologiske Tidsskrift 68, 75–87.

Schouenborg, B.E., 1989. Primary and tectonic basement-cover relationships in northernmost Vestranden, central Norwegian Caledonides. Norsk Geologiske Tidsskrift 69, 209–223.

Shelley, D., 1989. P, M and G tectonites: a classification based on origin of mineral preferred orientations. Journal of Structural Geology 11, 1039–1044.

Shelley, D., 1995. Asymmetric shape preferred orientations as shear-sense indicators. Journal of Structural Geology 11, 1039–1044.

Siddans, A.W.B., 1976. Deformed rocks and their textures. Philosophical Transactions of the Royal Society London, Series A 283, 43–54.

Siddans, A.W.B., 1977. The development of slaty cleavage in a part of the French Alps. Tectonophysics 39, 533–557.

Soto, J.I., 1991. Strain analysis using the maximum frequency of unimodal deformed orientation distributions: applications to gneissic rocks. Journal of Structural Geology 13, 329–335.

Talbot, C.J., 1970. The minimum strain ellipsoid using deformed quartz veins. Tectonophysics 9, 47–76.

Tucker, R.D., 1986. Geology of the Hemnefjord–Orkanger area, south-central Norway. Norsk Geologiske Undersøkelse Bulletin. 104, 1–21.

Tullis, T.E., 1976. Experiments on the origin of slaty cleavage and schistosity. Geological Society of America Bulletin 87, 745–753.

Tullis, T.E., Wood, D.S., 1975. Correlation of finite strain from both reduction bodies and preferred orientation of mica in slate from Wales. Geological Society of America Bulletin 86, 632–638.

Wheeler, J., 1989. A concise algebraic method for assessing strain in distributions of linear objects. Journal of Structural Geology 11, 1007–1010.

Wolfram, S., 1990. Mathematica: A System for Doing Mathematics by Computer. Addison-Wesley, Reading, MA.

Wood, D.S., Oertel, G., Singh, J., Bennett, H.F., 1976. Strain and anisotropy in rocks. Philosophical Transactions of the Royal Society London, Series A 283, 27–42.